

PROPOSED MODEL OF SHEAR DEFORMATION OF REINFORCED CONCRETE BEAM AFTER DIAGONAL CRACKING

Chayanon HANSAPINYO¹, Amorn PIMANMAS², Koichi MAEKAWA³ and Taweep CHAISOMPHOB⁴

¹Graduate Student

²Member of JSCE, Dr. Eng., Assistant Professor

⁴Member of JSCE, Dr. Eng., Associate Professor

Dept. of Civil Eng., Sirindhorn International Institute of Technology, Thammasat University
(P.O. Box 22, Thammasat Rangsit Post Office, Pathumthani, 12121, Thailand)

³Member of JSCE, Dr. Eng., Professor, Dept. of Civil Eng., University of Tokyo
(Hongo, Bunkyo-ku, Tokyo 113, Japan)

This paper presents the results of tests of four reinforced concrete beams with web reinforcement in order to measure the significance of shear deformation of the beams after diagonal cracking. The parameters affecting shear behavior, i.e. reinforcement ratio, shear span-to-depth ratio, and web reinforcement ratio were considered here. In addition, parametric study is performed by using the results of nonlinear finite element analysis and analytical model for predicting shear deflection is derived. The validity of the proposed model is made through the comparison with the above experimental results. It was found that the additional shear deflection computed using the present model agrees well with the experimental measurement.

Key Words : reinforced concrete beam, analytical model, diagonal cracking, shear deformation

1. INTRODUCTION

Since the deformation must be taken into consideration to provide the proper performance in normal service of the structures, the recent design of reinforced concrete member deals not only with strength but also with deformation. As a matter of fact, the member that is satisfied with the required strength may be subjected to excessively large deformation. Hence, many researches have been striving to establish a mathematical model for estimating deformation of reinforced concrete member.

In general, the calculation of deflection of reinforced concrete beam does not cover the component due to shear, as the shear deflection is negligible in most of the slender beams. However, short beam or beam with thin web subjected to large shear force requires a shear deflection calculation to be added to the deflection due to flexure. In addition, diagonal cracking may occur even under normal service condition and rapidly increases the shear deflection.

One of the well-known equations for prediction of reinforced concrete beam deflection has been developed by Branson¹⁾, and is based on interpolation of cracked and uncracked sectional stiffness. The equation gives a prediction of deflection of reinforced concrete member governed by flexural behavior. However, reinforced concrete member is generally incorporated with shear force, especially the inelastic shear deformation after diagonal cracking. In this case, since the equation excludes shear deflection, Branson's Equation underestimates member deflection.

The quantification of shear deformation in terms of geometry and mechanics of shear resistance is often represented by a truss model. The deformation computed includes shortening of a concrete strut and stretching of the vertical ties. The simplest way assumes diagonal crack inclination of 45 degrees²⁾. Ref.[3] has considered the effect of tension stiffness of concrete surrounding stirrup and direction of diagonal crack. However, the calculation using the truss mechanism does not consider effect of axial deformation due to flexure or axial force, only that

shear cracking force is adjusted in retarding or accelerating the commencement of diagonal cracking. Moreover, before the formation of diagonal cracking, flexural cracks have already been developed in the shear span. Hence, after flexural cracking, the shear stiffness is no longer in the elastic range. The test of shear transfer across pre-cracked specimens revealed the influence of crack width on the reduction of shear stiffness⁴. The nature of roughness in crack surface enables the shear stress to be transferred between the parallel planes. However, when the crack is opened wider, this capacity is reduced and hence shear stiffness decreases.

Based on the truss mechanism, diagonal shear crack enlarges axial deformation. The stress and strain in longitudinal bar will be higher than those predicted by flexural theory. As a result, there will be additional curvature due to shear crack, especially in the case of yielding of the longitudinal bar².

In this study, four reinforced concrete beams with web reinforcement are tested to carefully measure the deflection due to flexure and shear. On the other hand, the nonlinear finite element analysis of reinforced concrete panels is performed. The present analysis assumed that reinforced concrete beams are composed of number of small panels as shown in Fig.1, i.e. panels subjected to axial and shear loads or panels subjected to pure shear load. When the behavior of constituent panels is known, the whole behavior of the beams can be understood. The advantage of this method is the ability to perform the parametric study on the behavior of the beams affected by concrete compressive strength, content of longitudinal/transverse reinforcements and yielding strength of the reinforcement. Based on the results of the parametric study, a model to predict shear deflection of reinforced concrete beams accounting for shear stiffness deterioration due to flexural and diagonal cracking is established. Finally, this proposed model is verified by comparison with the present experimental results of four beams.

2. EXPERIMENTAL PROGRAM

(1) Experimental program

Four simply-supported reinforced concrete beams were tested under two concentrated loads, as shown in Fig.2, to study the factors influencing shear deformation i.e. shear span-to-depth, longitudinal reinforcement and web reinforcement contents. All specimens have 150 mm. by 350 mm. rectangular cross-section and 25-mm deformed bar was used for

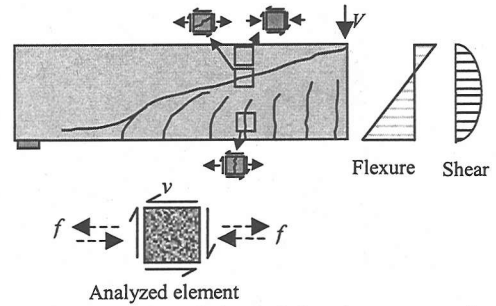
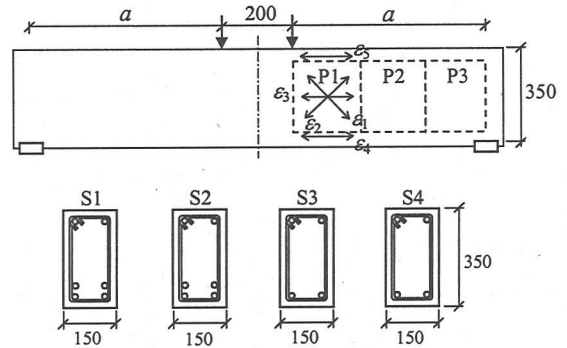


Fig.1 Parametric analysis of reinforced concrete panel



Unit: mm.

Fig.2 Dimension of test specimens

longitudinal reinforcement and 6-mm round bar for stirrup. The yielding strengths for longitudinal bar and stirrup are 440 MPa and 370 MPa, respectively. The parameters assigned to each specimen are shown in Table 1.

(2) Instrumentation

Load intensity applied at the middle span of specimens was measured by load cell of 50-ton capacity placed above the transfer I-section steel beam in order to apply two concentrated loads to the specimen. Electronic wire strain gauges were attached on longitudinal bars and stirrups to measure elongation of the steel. Regarding to surface deformation, on the concrete surface of specimens, the electronic transducers PI type (Fig.3) are used to measure the normal and shear strains of concrete surface based on the rosette concept.

Table 1 Specimens details

Specimen	f'_c (MPa)	ρ_l (%)	a/d	ρ_w (%)
S1	33	4.26	2.6	0.47(RB6@80 mm)
S2	33	4.26	3.5	0.47(RB6@80 mm)
S3	33	2.13	2.6	0.47(RB6@80 mm)
S4	33	2.13	2.6	0.31(RB6@120 mm)

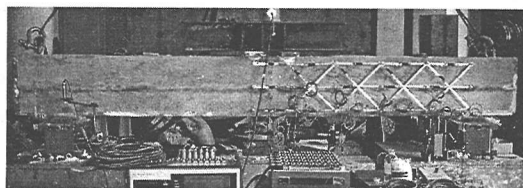


Fig.3 Test specimen: S2

Table 2 Shear capacities

Specimen	V_c (kN)	V_u (kN)	V_s (kN) ($V_u - V_c$)	V_n (kN)
S1	73.6	189.2	115.7	250.8
S2	64.1	175.6	111.5	185.7
S3	61.3	164.2	102.9	147.8
S4	61.6	132.4	70.8	147.8

The deflection of the beam is also measured by displacement transducers. The deformation measurements were performed only on one side of specimens (right side in Fig.3) which was controlled to fail by providing more shear reinforcement content on the other side.

(3) Measurement of shear deformation

Reinforced concrete specimen is visualized to be composed of reinforced concrete panels as shown in Fig.2 and deformation of each panel was measured by systematic arrangement of transducers PI-type. With the obtained two strains i.e. ϵ_1 , and ϵ_2 with 45-degree inclination to the beam axis, shear deformation can be calculated using strain transformation law. Hence, shear deflection at midspan can be obtained by summarizing shear deformation of each panel. Alternatively, shear deflection was obtained by subtracting the total deflection measured by a displacement transducer with flexural deformation calculated by double integration of curvature along the length of beams. The curvature is calculated from the measured deformation along the member axis i.e. ϵ_3 , ϵ_4 and ϵ_5 . Shear deflections obtained from these two approaches are compared to examine the consistency of the measurements and their average values are used in this study.

(4) Diagonal cracking strength

In this study, shear force at diagonal cracking is obtained by considering strain in stirrups. It was assumed that stirrup will never make contribution on shear resistance before the presence of diagonal cracking. The diagonal cracking strength is then

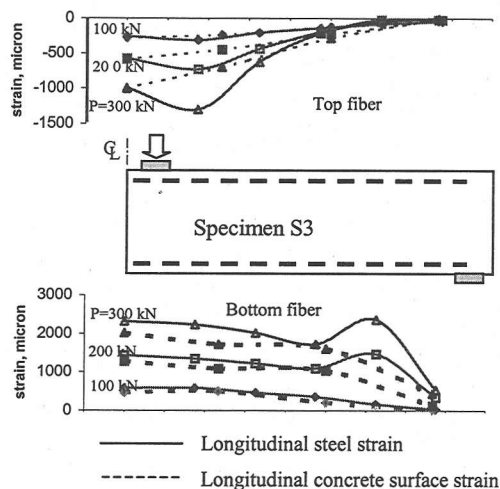


Fig.4 Axial deformation of beam S3

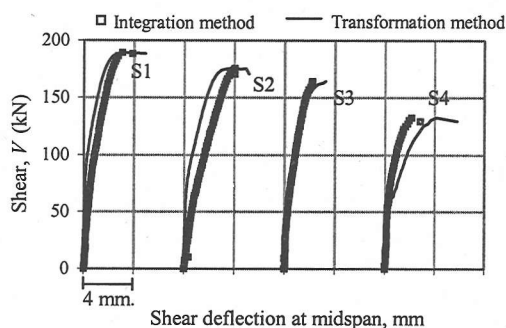


Fig.5 Separated shear deflection at midspan

defined as the shear force at the occurrence of stirrup strain at the middle of shear span. This diagonal cracking is also checked with the point on the relationship between shear force and shear strain where the shear stiffness starts decreasing.

3. EXPERIMENTAL RESULTS

(1) Capacity and failure behavior

Diagonal cracking capacity V_c as explained above, ultimate shear capacity V_u obtained from the experiment, shear reinforcement capacity V_s (taking the difference between V_u and V_c) and calculated flexure capacity V_n are given in Table 2.

Cracking initiation process agreed with those observed in the various past researches on shear test of reinforced concrete beam with moderate shear span-to-depth ratio. Similarity on crack generation for all specimens can be seen. First, typical flexural crack appeared at the flexural span. With continuous increase of load, the first flexural cracks extended

upwards and new flexural cracks were generated in shear span. It was then followed by diagonal cracks developed from the flexural cracks in shear span. At diagonal cracking load, the diagonal cracks propagated to the extreme top fiber of the beam. Failure state was reached when the extension of diagonal crack caused yielding of stirrups. This type of failure is classified as diagonal tension failure. However, yielding of extreme tension reinforcing bar of specimen S2 and S3 were seen before ultimate shear load, at applied shear load of 145.1 kN and 156.7 kN, respectively.

(2) Deformation of member

Deformation in longitudinal component measured in extreme tension and compression bars and concrete surface of the test specimen S3 are plotted in Fig.4. It can be seen that the longitudinal deformation from two measurements agrees well except at the locations near support and loading point in which jumping of longitudinal strain of reinforcements were observed. It indicates the localized deformation at the end tip of diagonal cracking path (top fiber) and large extension at the bottom fiber. As explained previously, the shear deflection can be obtained by two methods, i.e. integration of curvature and strain transformation of X-shaped PI-gauges. The comparison of shear deflection obtained from integration method and transformation method is made in Fig.5. Strain values obtained from strain gauges attached on the longitudinal reinforcements are locally measured at the gauge positions and ,therefore, the measured strains are dependent on the location of cracks. On the other hand, strain values obtained from PI-gauges are averaged over the gauge length. However, cracking passing through the contact points of the gauges may lead to measurement error. As seen in Fig.5, the difference in shear deflection can be seen from the two measurement methods and shear deflection of the specimens, for further discussion, are defined by using the averaged value.

(3) Midspan deflection

Fig.6 shows the relationship between applied load and measured midspan deflection of the tested specimens. Before flexural cracking, the behavior obeys elastic theory. After the occurrence of flexural cracking, the stiffness is decreased. With the continuous increase of load, diagonal crack occurs and leads to the further reduction of member stiffness.

The total deformation shown in Fig.6 includes deflection due to flexure and deflection due to shear.

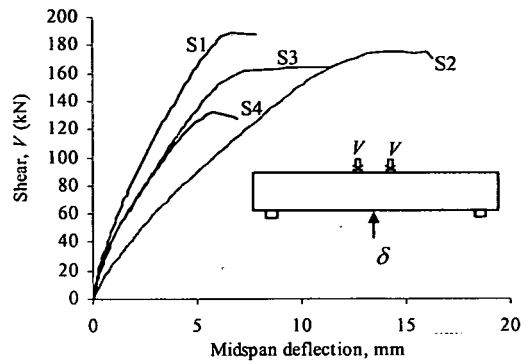
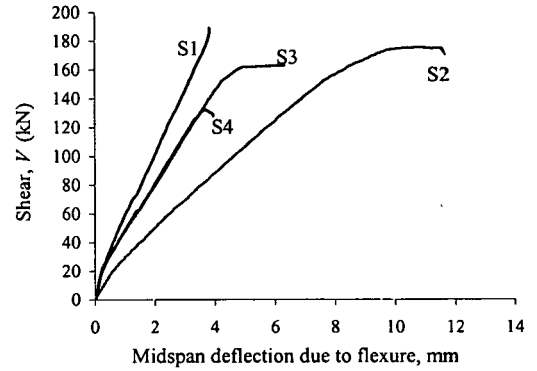
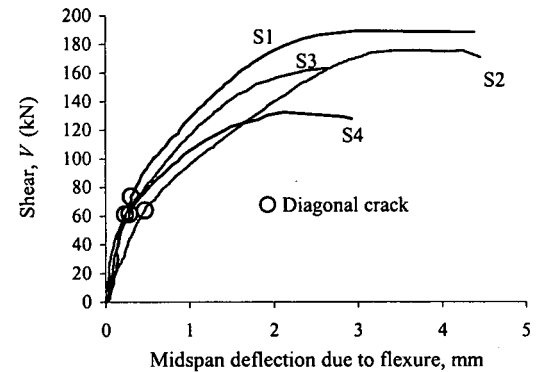


Fig.6 Observed load-mid span deflection



(a) Separated flexural deflection at midspan



(b) Separated shear deflection at midspan

Fig.7 Separated deflection at midspan

In order to identify how beam parameters affect shear deformation, separation of two types of deflection is performed. Figs.7(a) and (b) show the separated flexural and shear deflection, respectively.

The significance of shear deflection of the tested reinforced concrete beams is considered as shear-to-total deflection ratio or flexural-to-total deflection ratio, as shown in Fig.8. It can be seen that, the flexural deflections at early load state (state

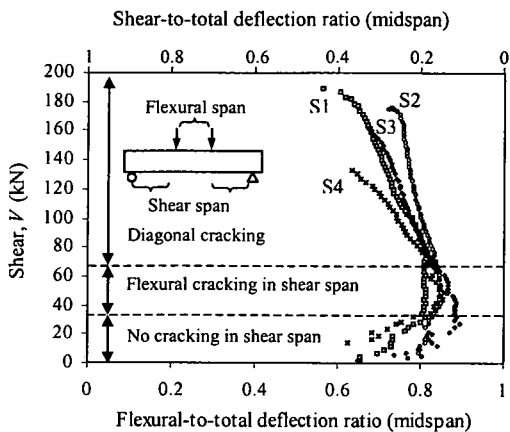


Fig.8 Ratio of flexural-to-total deflection at midspan

of no cracking in shear span) are scattering between 60 to 80 percent of the total deflection measured at midspan. With the increase of applied load, flexural cracks were developed in the flexural span but no crack in shear span. At this state, flexural stiffness was reduced while shear stiffness in shear span remained constant as initial. Accordingly, flexural deflection was increased at the rate faster than the increasing of shear deflection. Hence, the ratio of flexural-to-total deflection was increased in this applied load range. However, once the flexural crack propagated in shear span, the ratio is likely constant at approximately 0.85. It implies that the increasing rate of flexural and shear deflections are almost equal up to the diagonal cracking load. Afterwards, the flexural-to-total deflection ratio reduced. It indicated that the increasing rate of shear deflection is faster than flexural deflection. In other words, the shear deflection is much increased due to diagonal cracking. Comparisons among the four tested beams, specimen S2 has the largest deflection for both due to flexure and shear, however, the deflection due to shear at ultimate load on specimen S2 is only 25 percent of the total deflection, which is the smallest one. For the specimen S1 which has a total deflection less than that of beam S2, the deflection due to shear at ultimate is as high as 44 percent of the total deflection. The significance of shear deflection of specimen S3 and S4 at ultimate are 33 and 37 percent of the total deflection, respectively.

(4) Effect of shear span-to-depth ratio

Specimens S1 and S2 contain similar properties except that shear span-to-depth ratio of S1 is 2.6 while that of S2 is 3.5. From Figs.6 and 7, the specimen S2 with larger shear span-to-depth ratio has more deflection due to shear and flexure than the specimen S1. However, as can be seen in Fig.8, the

significance of shear deflection is smaller in case of specimen S2.

The shear span-to-depth ratio is actually the ratio of moment-to-shear, and the moment exerts the axial deformation of the beam. Hence, for the beam with higher shear span-to-depth ratio, the axial deformation is higher, and consequently flexural deflection tends to increase. Moreover, specimen S2 has longer shear span compared to specimen S1.

Regarding cracking behavior with different shear span-to-depth ratio, the potential diagonal tension crack of specimen with higher shear span-to-depth ratio propagates more rapidly than that of specimen having the lower ratio⁵. This cracking behavior agrees with the conclusion that the higher the shear span-to-depth ratio the higher shear deflection. In addition, as observed in the test, the critical diagonal crack propagated at lower degree of inclination compared to specimen S1. Based on the equilibrium of truss mechanism, this leads to the higher additional axial deformation which will be discussed further.

(5) Effect of longitudinal reinforcement content

In order to examine the effect of longitudinal reinforcement, specimens S1 and S3 are compared. Specimen S1 contains 4.26% of longitudinal reinforcement and 2.13% for specimen S3. As shown in Fig.7, less longitudinal reinforcement of specimen S3 i.e. smaller flexural stiffness results in larger axial deformation and hence flexural deflection and shear deflection increase. However, the significance of shear deflection to the total deflection of specimen S1 and S3 is almost the same as shown in Fig.8.

Based on shear resisting mechanism, the longitudinal reinforcement also directly provides shear resistance in the term of dowel action. Moreover, the tensile restraint itself helps development of aggregate interlocking.

(6) Effect of web reinforcement content

Deformation responses of specimen S3 and S4 indicate the effect of web reinforcement content to shear deflection. Percents of web steel reinforced are 0.47% for specimen S3 and 0.31% for specimen S4. Since the same longitudinal reinforcement is provided for these two specimens, no difference in flexural deflection can be observed in Fig.7a. Before the initiation of diagonal cracking as shown in Fig.7b, shear deflections of two beams agree well. However, shear deflection of specimen S4 increases more rapidly than that of S3 after the occurrence of diagonal cracking. Placing higher content of stirrup in shear span results in reduction of shear deflection at the same shear force. The reason is that critical

shear crack is more stable and hence the propagation of the crack is retarded. In the test, the crack propagation of specimen S4 is faster and develop fewer cracks than that of specimen S3. It is obviously seen that, however, the ultimate capacity of specimen S3 with higher content of shear reinforcement is higher and consequently the longer time of developing shear deflection. Therefore, as shown in Fig.8, even the higher shear stiffness after diagonal cracking of specimen S3 compared to that of specimen S4, the ultimate shear deflection of specimen S3 is 33 percent of the total deflection which is slightly lower than that of 37 percent of the total deflection of specimen S4.

(7) Additional curvature due to diagonal cracking²⁾

It is apparently shown from Fig.9 that after diagonal cracking, there exists the deviation of the measured flexural deflection from the calculation by using Branson’s equation or ACI specification¹⁾. This is due to the additional axial force exerted after diagonal cracking²⁾, as expressed in Eq.(1).

$$\Delta T = \frac{V_s (\cot \theta - \cot \alpha)}{2} \quad (1)$$

where

- ΔT is additional tensile force of longitudinal reinforcement after diagonal crack
- V_s is shear reinforcement capacity
- θ is inclination angle of diagonal crack
- α is inclination angle of stirrup

This additional tensile force results in an additional strain $\Delta \epsilon_{sl}$ of the longitudinal reinforcement. If the assumption of plane section is retained the additional curvature $\Delta(1/r)$ produced by $\Delta \epsilon_{sl}$ can be estimated by

$$\Delta(1/r) = \frac{\Delta \epsilon_{sl}}{z} \quad (2)$$

where

z is lever arm of internal forces

By using the double integration method and assuming uniform distribution of additional curvature along the shear span with 45-degree (θ) inclination angle of diagonal crack²⁾, additional flexural deflection can be obtained. As shown in Fig.9, including additional curvature after diagonal cracking in the calculation improves the prediction of deflection due to flexure.

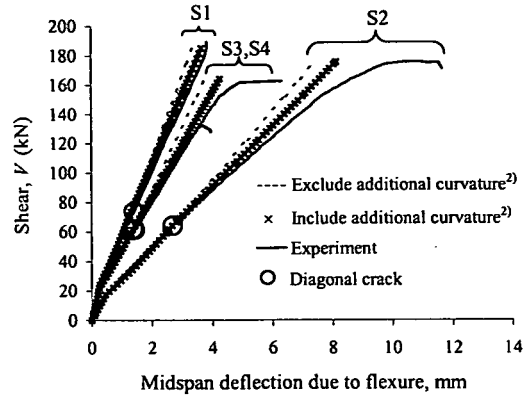


Fig.9 Additional flexural deflection after diagonal cracking

4. SHEAR DEFORMATIONAL MODEL

Due to the lack of experimental database regarding shear deformational behavior of reinforced concrete member, this study will adapt an analytical approach. As discussed in Chapter 1, INTRODUCTION and Fig.1, the nonlinear finite element analysis of three types of reinforced concrete panels subjected to pure shear, combined shear and axial compression, and combined shear and axial tension, is performed by changing ratio of applied shear and axial forces to the panels. The parameters considered here are material properties i.e. concrete compressive strength (20-60 MPa), yielding strength (240-400 MPa) and amount of longitudinal and transverse reinforcements (0.1-10% each). Based on the analytical results, a model for shear deformation of reinforced concrete beam according to cracking behavior is derived. The analytical tool used here is nonlinear finite element program named WCOMD which is developed by the Concrete Laboratory, of The University of Tokyo. Constitutive laws for concrete and reinforcement under compression, tension and shear are described in Ref.[6]. Performing analysis of reinforced concrete panel subjected to pure shear with varying concrete strength and keeping reinforcement content as constant as 1% both in longitudinal and transverse (web reinforcement for beam) directions, Fig.10. shows the influence of concrete strength on shear deformation behavior. When the concrete strength is higher the shear stiffness becomes higher. Three types of loading of specimens having 1% reinforcement content both in longitudinal and transverse directions with varying axial-to-shear forces ratio (f/v) and concrete strength of 20 Mpa, 30 Mpa and 60 MPa, plot of normalized shear stiffness, which is defined by the reduced shear stiffness after cracking (G)-to-elastic shear stiffness (G_e) ratio

with axial strain is shown in Fig.11. It can be seen that, the degradation of the normalized stiffness of specimens with different concrete strength when plotting against axial deformation are similar and hence the expression for the effect of concrete strength on the shear stiffness degradation can be well represented by the normalized term. In Fig.12, the shear responses of analytical specimens containing different amount of reinforcement with constant concrete strength of 30 Mpa, subjected to pure shear loading, are shown. It can be seen that, the higher reinforced specimen shows the higher shear stiffness. Fig.13 illustrates the normalized shear stiffness affected by axial deformation of specimen with different amount of reinforcement contents, keeping concrete strength of 30 MPa. The first and second numbers labeled in the graph respectively mean percentage of transverse and longitudinal reinforcements. The figure indicates that the specimen with the same content of transverse reinforcement but difference in longitudinal reinforcement ,i.e. the specimens labeled as 1:1 and 1:5, and 5:1 and 5:5, have almost the same shear stiffness for each case. Hence, the influence of longitudinal reinforcement can be well represented by axial deformation. Upon this information, the normalized shear stiffness can be expressed as the function of the axial deformation and amount of transverse reinforcement. The study of reinforced concrete panels subjected to various ratios of axial-to-shear load reveals that the shear stiffness degradation after cracking is mainly affected by the occurrence of crack which reduces to approximately 20-30 percent of the initial elastic shear stiffness and magnified by the increasing of axial tension or decreased by axial compression, as shown in Fig.14. In case that the cracking is incorporated with the large axial tension especially after yielding of longitudinal reinforcement, shear stiffness is quite low which is about 3 percent of the initial one. Then, using the regression analysis, the empirical formula to predict shear stiffness after diagonal cracking is proposed in Eq.(3). For the calculation of shear stiffness before cracking, shear stiffness is followed elasticity. It is noted for Eq.(3) that the lower limit of G/G_e is set to be 0.03 when the value is less than 0.03. In addition, as adopted in the analysis, the equation is applicable for the range of shear reinforcement of 0.1 to 10% and no case of without shear reinforcement ($\rho_w=0$).

$$G/G_e = -68400\varepsilon_a^2 - 130\varepsilon_a + \left(140 - \frac{139.79}{\rho_w^{0.00028}}\right) \quad (3)$$

where

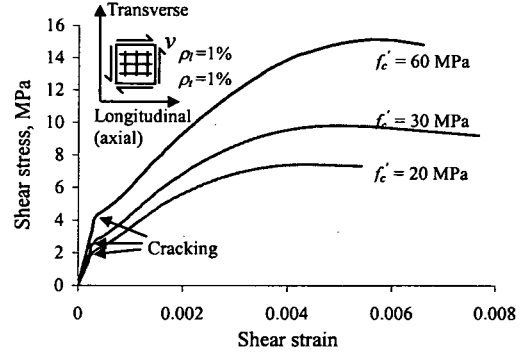


Fig.10 Shear response of reinforced concrete panel with different concrete compressive strength $\rho_t=1\%, \rho_l=1\%$ (constant)

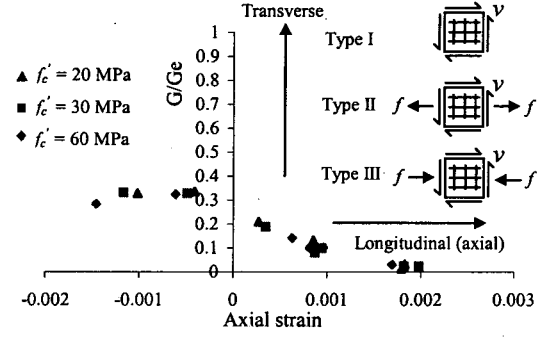


Fig.11 Degradation of shear stiffness with axial deformation of panel with different concrete compressive strength

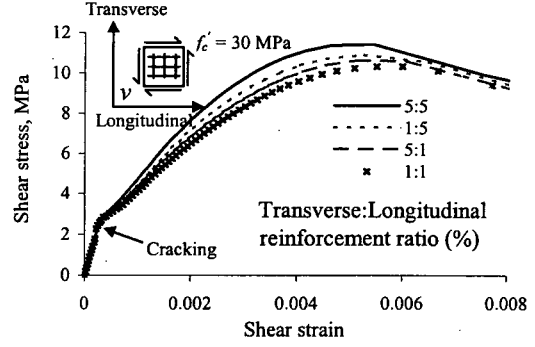


Fig.12 Shear response of reinforced concrete panel with different amount of reinforcement

G is reduced shear stiffness due to cracking
 G_e is elastic shear stiffness ε_a is axial strain
 ρ_w is percentage of shear (web) reinforcement

As shown in Figs.10 and 12, the shear deformational behavior of reinforced concrete panel can be divided into two states upon cracking, i.e. before and after the cracking. However, in reinforced concrete beam, cracking patterns involving nonlinear deformational behavior are classified as flexural and

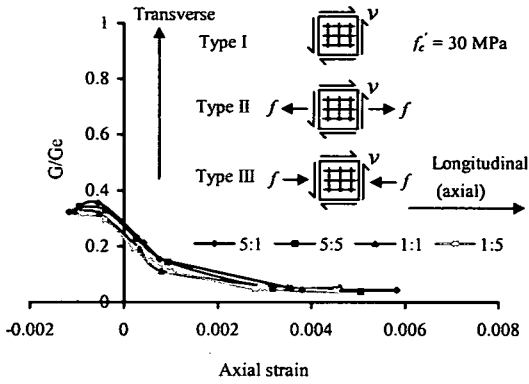


Fig.13 Degradation of shear stiffness with axial deformation of panel with different content of reinforcement

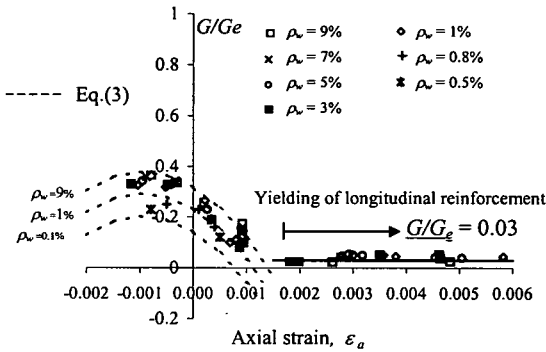


Fig.14 Shear rigidity degradation due to axial deformation after cracking (a part of data are plotted)

diagonal shear cracks. Typically, flexural cracking has been initiated before diagonal cracking. Hence, shear deformational behavior of reinforced concrete beam is divided into three ranges as shown in Fig.15, i.e. uncracked, after flexural cracking and before diagonal cracking in shear span, and after diagonal cracking. The adoption of the derived model to calculate shear deflection of reinforced concrete beam according to the three states is described as follows:

(1) State 1: Uncracked elastic state

Before the presence of flexural cracks, i.e. in the elastic range, the shear stress is well related to shear strain with shear modulus as shown below,

$$G_e = \frac{E_c}{2(1 + \mu)} \quad (4)$$

where E_c is Young's modulus and μ is Poisson's ratio of concrete, which is approximately 0.16 to 0.30 for normal weight concrete. The cross sectional shear stiffness relating shear force and shear strain, γ ,

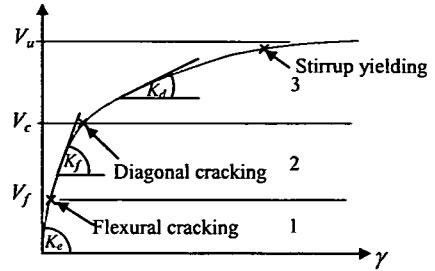


Fig.15 Three states of shear deformational behavior of reinforced concrete beam

is obtained by multiplying shear modulus, as shown in Eq.(4), with shearing surface bd . With the assumption of plane section remains plane after deformation, the stiffness is modified with the form factor for shear f_s , in which it can be taken as 1.2 for the rectangular section. Eq.(5) shows the sectional shear stiffness providing elastic shear deformation.

$$K_e = \frac{G_e bd}{f_s} \quad (5)$$

Hence, shear deformation can be directly computed as, with taking $G_e = 0.4E_c$ i.e. Poisson's ratio is 0.25.

$$\gamma_e = \frac{V * f_s}{0.4E_c bd} \quad (6)$$

(2) State 2: After flexural cracking and before diagonal cracking

Under load increase, flexural cracks developed in shear span. The extension of the flexural cracks reduces shear transfer capacity and consequently shear rigidity. The effect of the flexural crack on the sliding plane of shear transfer may be explained by test of pre-cracked concrete under sliding shear⁴⁾. The study reported that with the increase of crack width, shear stress transferred by aggregate interlocking mechanism is reduced. Accordingly, the generation of flexural crack then reduces not only the flexural stiffness but also capability in transferring shear force of member. Sato et. al.³⁾ adopted the expression for estimating effective flexural stiffness, which is termed as third power of cracking moment-to-applied moment ratio, to calculate the effective cross-sectional area for shear rigidity accounting the influence of the flexural cracking. In this study, the effect of flexural cracking on shear stiffness degradation is taken into account by considering the expression in Eq.(3). As shown in Fig.15, the cross sectional shear stiffness in this state is represented by K_f .

(3) State 3: After diagonal cracking

When shear force is increased to the shear cracking strength, two planes of the crack tend to slide from each other. The sliding of the diagonal crack plane causes a large shear deflection of the member and reduces the cross sectional shear stiffness to K_d , as shown in Fig.15. The occurrence of diagonal cracking considerably differs the reinforced concrete beam behavior from that prior to the cracking. In other words, the magnitude of shear deflection depends largely on the formation of diagonal shear cracks. The calculation of shear stiffness after diagonal cracking uses the model shown in Fig.14 and Eq.(3).

Even the same model in Eq.(3) and Fig.14 is adopted for the calculation of shear modulus in state 2 and 3, the following reasons are made to distinguish the result between two states. In state 2, the behavior is governed by flexure which can be explained based on sectional behavior. Subject to positive bending moment, a reinforced concrete beam is generally cracked from bottom fiber to top fiber in the vertical direction. Hence, the concrete in compression zone can be treated as uncracked concrete and the concrete in tension is treated as cracked concrete. Then by layer formulation, the elastic shear modulus in Eq.(4) is used in the compression zone, and the reduced shear modulus in Eq.(3) is used in the tension zone. On the other hand, after diagonal cracking in state 3, the behavior of the member is shifted from sectional response to somewhat member response. In shear span, the diagonal cracks propagate from the bottom part near beam supports to the top part close to loading points. Since, many diagonal cracks of reinforced concrete beam with shear reinforcement are generated in shear span after diagonal load, it is then assumed that the diagonal cracks are smeared throughout the whole part of shear span, and hence reduced shear modulus in Eq.(3) is used throughout the section.

5. MODEL VERIFICATION

(1) Reinforced concrete panels

The first level of verification is performed at a layer or panel level of reinforced concrete beam, i.e. panels are subjected to axial and shear loads or pure shear load as shown in Fig.1 The comparison is made between the shear responses calculated by the proposed shear deformational model in this study and those of the tested panels. The tested reinforced concrete panels by Vecchio and Collins⁷⁾ are selected

here and were subjected to pure shear or combined shear and bi-axial loading. The specimens selected are monotonic loading and failed in concrete cracking or yielding of reinforcement.

The tested specimens are divided into 2 series in accordance with loading scheme. Series 1 is subjected to pure shear and composed of 2 groups. Specimens in Group I were identically reinforced in longitudinal and transverse directions while different for specimens in Group II. Specimen PV26 was pretensioned before applying monotonic pure shear. Properties of specimen in Series 1 are shown in Table 3.

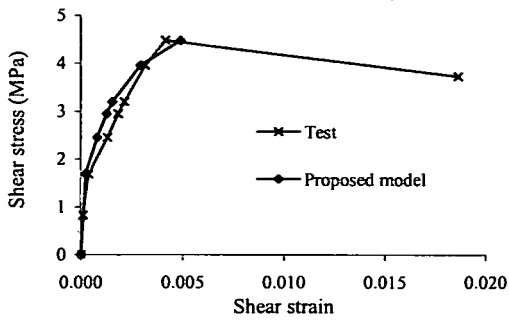
The test Series2 is comprised of four panels which were tested under combination of shear and biaxial stresses by keeping the ratio of biaxial stresses-to-shear, f_n/v , as constant. Details of the four panels are listed in Table 4.

Table 3 Series 1 test panels (pure shear stress)

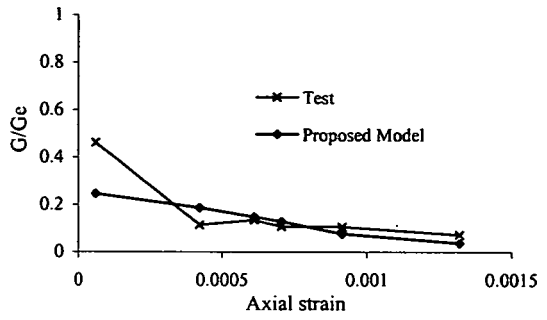
Group	Specimen	Longitudinal reinforcement ratio (ρ_l)	Transverse reinforcement ratio (ρ_t)	f'_c (MPa)
I	PV2	0.00183	0.00183	23.5
	PV4	0.01056	0.01056	26.6
	PV6	0.01785	0.01785	29.8
	PV9	0.01785	0.01785	11.6
	PV16	0.00740	0.00740	21.7
II	PV10	0.01785	0.00999	14.5
	PV11	0.01785	0.01306	15.6
	PV12	0.01785	0.00446	16.0
	PV18	0.01785	0.00315	19.5
	PV19	0.01785	0.00713	19.0
	PV20	0.01785	0.00885	19.6
	PV21	0.01785	0.01296	19.5
	PV22	0.01785	0.01524	19.6
	PV26	0.01785	0.01009	21.3
	PV27	0.01785	0.01785	20.5

Table 4 Series 2 test panels (combined shear and bi-axial stresses)

Specimen	Longitudinal reinforcement ratio ρ_l	Transverse reinforcement ratio ρ_t	f'_c (MPa)	f_n/v
PV23	0.01785	0.01785	20.5	-0.39
PV24	0.01785	0.01785	23.8	-0.83
PV25	0.01785	0.01785	19.2	-0.69
PV28	0.01785	0.01785	19.0	0.32

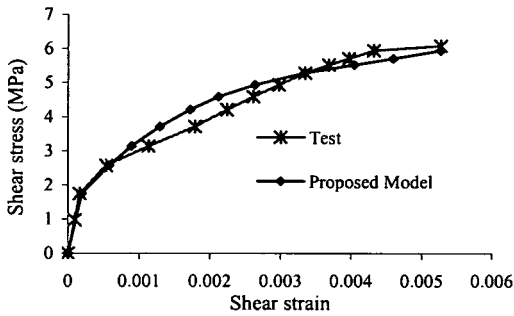


(a) Shear stress-shear strain relationship of PV6

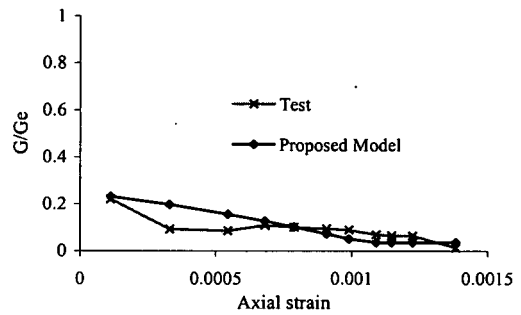


(b) Shear stiffness -axial strain relationship of PV6 after diagonal cracking

Fig.16 Shear stress-shear strain relationship and degradation of shear stiffness related to axial deformation of PV6

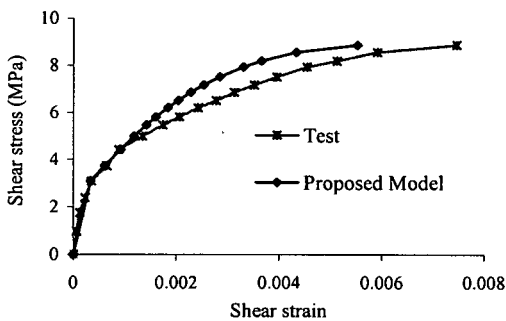


(a) Shear stress-shear strain relationship of PV22

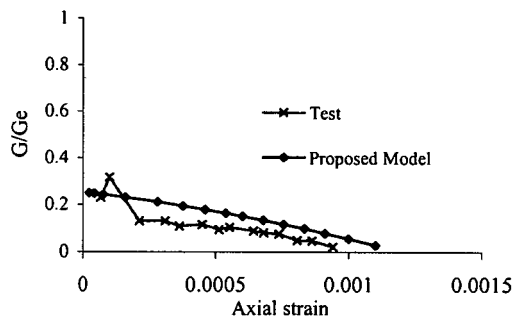


(b) Shear stiffness-axial strain relationship of PV22 after diagonal cracking

Fig.17 Shear stress-shear strain relationship and degradation of shear stiffness related to axial deformation of PV22



(a) Shear stress-shear strain relationship of PV23



(b) Shear stiffness-axial strain relationship of PV23 after diagonal cracking

Fig.18 Shear stress-shear strain relationship and degradation of shear stiffness related to axial deformation of PV23

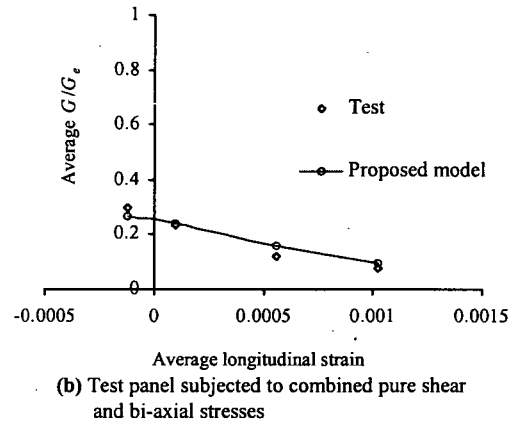
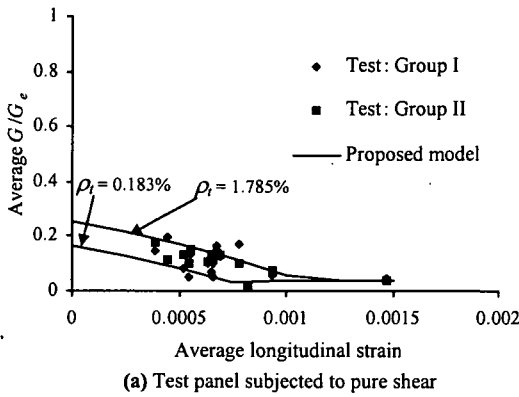


Fig.19 –Normalized shear stiffness

Figs.16-18 respectively show the shear stress-shear strain relationships and shear stiffness degradation with the axial deformation of panels PV6, PV22 and PV23 obtained from the present shear deformational model and from experiments. The calculation is divided into two states, i.e. uncracked elastic state and cracked state. At the first state, elastic behavior is assumed and the calculation follows the expressions in Eqs.(4)-(6). In the second state, the proposed model in Eq.(3) is adopted. Axial strain observed from the test corresponding to applied shear stress is used to estimate shear stiffness of the panels. In addition, plot of averaged shear stiffness after diagonal cracking with longitudinal strain of all specimens are shown in Fig.19 together with calculation using the model. It can be seen that the shear stiffness of reinforced concrete panel can be well predicted by using the proposed model.

(2) Reinforced concrete beam

The verification at a member level is made through the four tested beams in above section. Midspan deflection measured from the tests are compared with the calculation ones. The calculated beam deflection is obtained by taking superposition of deflection due to flexure and deflection due to shear. The ACI design specification adopting evaluation of effective flexural stiffness EI_{eff} proposed by Branson¹⁾ is used to compute the first type of beam deflection. The calculation for deflection due to shear of reinforced concrete beam uses the proposed model. Due to the distribution of axial deformation across section about the neutral surface, the cross section is divided into small layers and taking mean strain in each layer to estimate shear stiffness(5 layers in this calculation, as shown in Fig.20). As the results of the analysis of reinforced concrete panels, the influence of longitudinal reinforcement

on shear deformation is described by axial strain. Large content of longitudinal reinforcement results small axial strain and small shear deformation. For a reinforced concrete beam, providing the longitudinal reinforcement increases flexural stiffness, decreases curvature and, hence, decreases axial strains in each layer. When the axial strains in each layer is reduced, from Eq.(3), shear stiffnesses of the layers become higher. Regarding shear reinforcement, the area of reinforcement is averaged over the shear span. Then, the proposed model in Eq.(3) is adopted to calculate shear stiffness in each layer and combining shear stiffness for each layer becomes sectional shear rigidity. The effect of addition curvature after diagonal cracking, which increases the axial deformation, is taken into account. For a typical reinforced concrete beam, as stated above, the calculation for shear deflection of reinforced concrete beam is divided into three steps regarding the cracking behavior of reinforced concrete beam, as follows (Fig.21);

(a) Before flexural cracking

Before the initiation of flexural cracking in shear span, elastic shear sectional stiffness is related to concrete Young's modulus E_c as described above regardless of axial strain distribution. Shear deflection at midspan is obtained by multiplying shear deformation angle obtained by Eq.(6) to the shear span as shown in Fig.21(a).

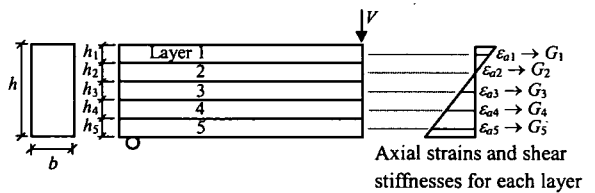


Fig.20 –Calculation of shear stiffness with 5- layer beam

(b) After flexural cracking and before diagonal cracking

The increase of shear force increases bending moment developed in shear span. When the applied moment has been developed over cracking moment, flexural cracks will be generated. The propagation of the flexural cracks inside shear span at the shear force below diagonal cracking strength depends on relative magnitude of flexural cracking shear V_c and cracking moment M_{cr} . For the case of simply-supported beam under two concentrated loads, if the diagonal shear strength is known, the span length free from flexural disturbance a_1 and the span length containing flexural cracking prior to diagonal cracking a_2 can be obtained as shown in Eq.(7).

$$a_1 = \frac{M_{cr}}{V_c} \quad (7a)$$

$$a_2 = a_0 - a_1 \quad (7b)$$

The calculation in this load range is subdivided into two steps according to the separated two shear lengths. The first is shear deflection in span length a_1 which is assumed to be elastic, and the calculation resembles the calculation in the elastic range 1. The second step is the calculation in span length a_2 . The effect of flexural cracking to shear stiffness will be taken into consideration in the calculation. The calculation in each layer is performed by taking strain gradient due to flexure at middle span length a_2 . The calculation of layers containing no crack or in the compression zone and some in tension zone adopts Eq.(6). For the layers possessing tensile strain larger than cracking strain in the tension zone, the model accounting for shear stiffness degradation after cracking shown in Fig.14

and Eq.(3) is used. Finally, combination of shear deflection exerted in the span length a_1 and a_2 gives shear deflection at midspan (Fig.21(b)).

(c) After diagonal cracking

When the applied external shear load reaches diagonal shear strength of specimen, diagonal crack occurs. The crack propagates both upward to compression zone at loading point and downward to tension zone at support and the beam is separated into two parts. The effect of shear force makes sliding of the two parts along the crack face. The shear deflection at this state is calculated by considering all shear span a_0 to be affected by this diagonal cracking. For the case of reinforced concrete beam subjected to two concentrated loads, bending moment generated in shear span varies linearly from support to loading point. Hence, without expected significant difference and to ease the calculation, axial strain at mid-shear span calculated from bending deformation is used to estimate the shear stiffness. Likewise, effect of strain gradient is considered by dividing the beam cross section into small layers.

Figs.22 and 23 respectively show the comparisons between the calculated shear and total deflections with measured deflections at midspan. The example of the shear deflection calculation of specimen S1 is shown in Table 5. The calculations for total deflection use the superposition of flexural deflection using Branson's equation and shear deflection using the proposed model. It can be seen that the calculation using model improves estimation of total deflection of reinforced concrete beam critical in shear.

Table 5 Calculation for shear deflection of specimen S1

Layer	$\rho_w(A_w/bs)^1$, %	Axial strain (ϵ_a)			G, MPa			K (Gbh/f_s), kN		
		State 1 ³	State 2	State 3	State 1 ³ (Eq.(4))	State 2 (Eq.(3))	State 3 (Eq.(3))	State 1 ³ (K_e)	State 2 (K_f)	State 3 (K_d)
1	4.71E-01	$\epsilon_{a5} < f_t/E_c^2$	-1.35E-04	-4.14E-04	9.28E+03	9.28E+03	2.26E+03	4.06E+05	8.12E+04	1.98E+04
2	4.71E-01		2.80E-05	1.57E-04		9.28E+03	1.67E+03		8.12E+04	1.46E+04
3	4.71E-01		1.91E-04	7.27E-04		1.62E+03	6.59E+02		1.41E+04	5.77E+03
4	4.71E-01		3.55E-04	1.30E-03		1.36E+03	2.79E+02		1.19E+04	2.44E+03
5	4.71E-01		5.18E-04	1.87E-03		1.08E+03	2.79E+02		9.41E+03	2.44E+03
					Total	4.06E+05	1.98E+05	4.51E+04		

¹ A_w is area of stirrup, b is beam width, s is stirrup spacing.

²Axial strain of the extreme tension layer (ϵ_{a5}) is less than cracking strain defined by f_t/E_c , where f_t is tensile strength and E_c is Young's modulus of concrete.

³Regardless of axial strain

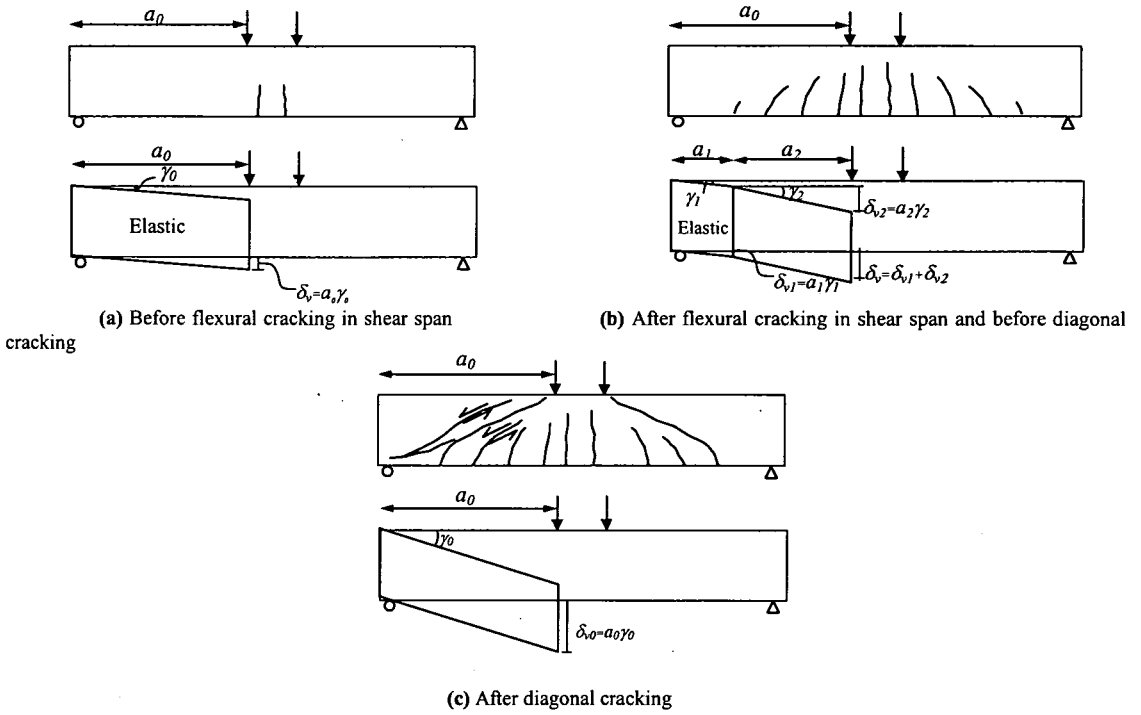


Fig.21. Calculation of shear deflection of reinforced concrete beam

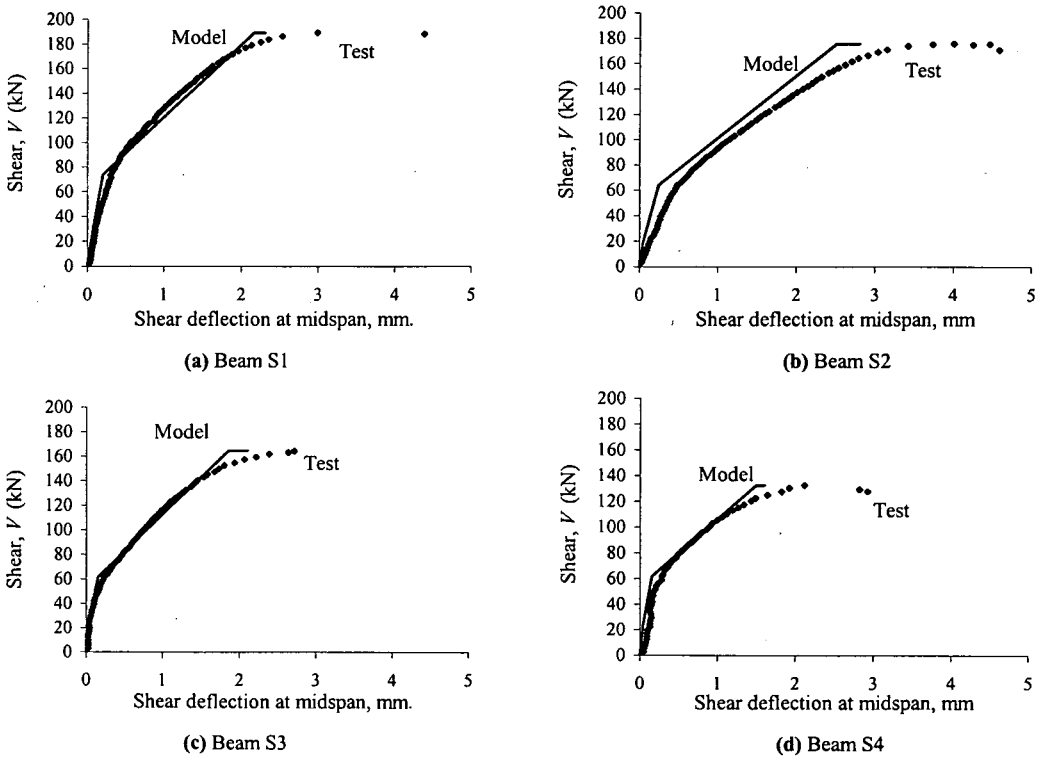


Fig.22 Comparisons on shear deflection at midspan

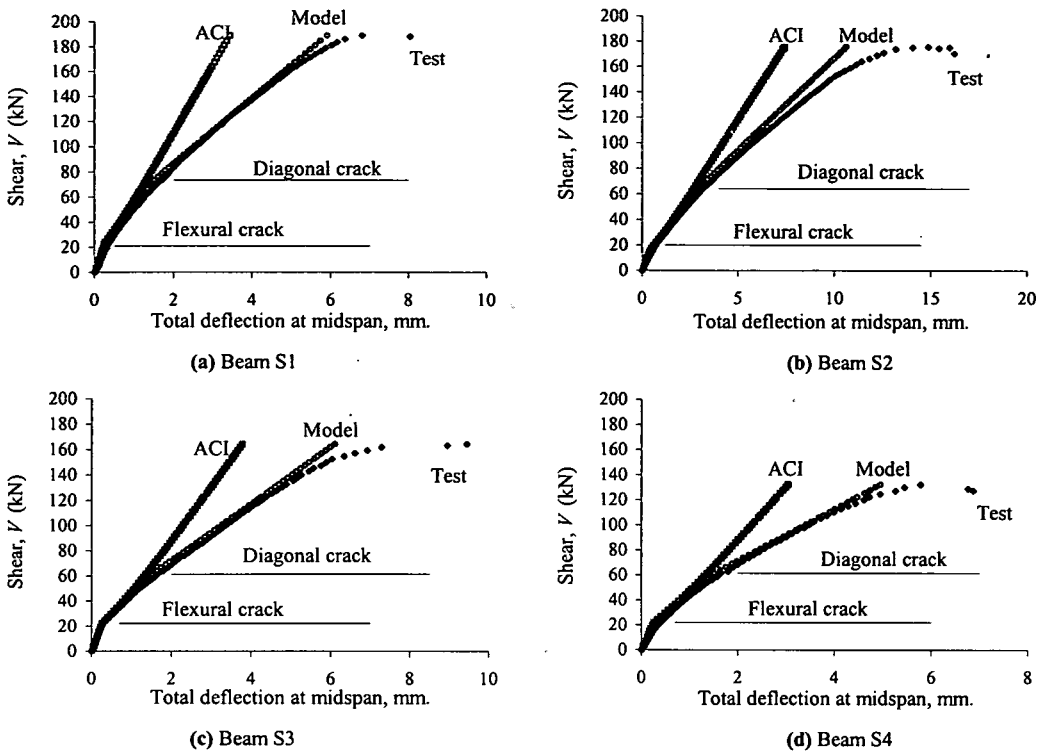


Fig.23 Comparisons on total deflection at midspan

6. CONCLUDING REMARKS

The following are the concluding remarks drawn up in this study.

1. Four reinforced concrete beams were tested in order to investigate effects of the following parameters on shear deformation, i.e. shear span-to-depth ratio, amount of longitudinal and shear reinforcements. It can be seen from the experimental results that at the same applied shear force the shear deflection is high when the shear span-to-depth ratio is high and content of longitudinal and shear reinforcements are low.

2. Based on the analysis of reinforced concrete panel, the shear deformation is mainly affected by the occurrence of concrete cracking which will decrease in shear stiffness from the initial elastic one by 20 to 30 percent. The stiffness degradation is then magnified by the presence of axial tensile strain or decreased by the axial compressive strain. By performing nonlinear finite element analyses of reinforced concrete panels as constituents of a reinforced concrete beam, the parameters affecting the shear modulus after concrete cracking are studied, and finally the empirical formula to predict

the shear modulus in terms of relationship between the ratio of reduced and initial shear modulus and the axial strain is proposed.

3. The calculation of shear deflection using the proposed model was first verified with the test of 19 reinforced concrete panels by Vecchio and Collins⁷. The comparisons indicates the accuracy of the model to estimate shear deformation in a layer level of reinforced concrete beam.

4. To calculate shear deflection of reinforced concrete beam, cross section is divided into layers. By using this approach, the strain gradient distributing over beam cross section influencing shear deformation can be simulated and the reduced shear modulus of the section can be obtained by using the proposed model, then the shear deflection of the reinforced concrete beam taking account of flexural and diagonal cracking can be predicted. The calculation of shear deflection proposed in this study seems to yield the results fit well with the experiments. Hence, the estimated total deflection can be improved by supplement the presently proposed calculation of deflection due to shear to the flexural deflection calculated by Branson's equation.

ACKNOWLEDGMENT: The authors would like to express their appreciation to The Thailand Research Fund for financial support under RGJ_Ph.D. Program.

REFERENCES

- 1) Branson, D. E.: *Deformation of Concrete*, McGraw-Hill, New York, 1977.
- 2) Comité Euro-International du Béton: *CEB Manual-Cracking and Deformations*, Ecole Polytechnique Fédérale de Lausanne, 1985.
- 3) Sato, Y., Ueda, T., Kakuta, Y.: Proposal for Deformational Model of Reinforced Concrete Beams, *ICCMC/IBST 2001 International Conference on Advanced Technologies in Design, Construction and Maintenance of Concrete Structures*, pp. 172-175, 2001.
- 4) Paulay, T. and Loeber, P.J.: Shear Transfer by Aggregate Interlock, *ACI SP-42*, Vol.1, pp.1-15, 1974.
- 5) Kim, W. and White, N R.: Shear-Critical Cracking in Slender Reinforced Concrete Beams, *ACI Structural J*, No.96, pp. 757-765, 1999.
- 6) Okamura, H. and Maekawa, K.: *Nonlinear Analysis and Constitutive Model of Reinforced Concrete*, Giho-do Press, Tokyo, 1991.
- 7) Vecchio, F.J. and Collins, M. P.: *The Response of Reinforced Concrete to In-Plane Shear and Normal Stresses*, Publication No.82-03, Department of Civil Engineering, University of Toronto, 1982.

(Received February 6, 2002)